Similarities and Differences when Solving Helmholtz Problems with Schwarz Domain Decomposition and Multigrid

Martin J. Gander[0000−0001−8450−9223],
Yafei Sun[0009−0008−7512−9550]

1 Introduction

The Helmholtz equation is a fundamental model for time-harmonic wave propagation, and its numerical solution has been extensively studied; see [9, 5, 12, 10] for domain decomposition, and [6, 7, 13, 8, 1] for multigrid. Recently, an analysis for the 2D Helmholtz equation on a bounded domain revealed that the convergence factor of Schwarz methods is strongly influenced by the outer boundary conditions (BCs) [11]: convergence for free space problems is much better than for cavity problems. For multigrid as an iterative method of equal importance, a natural question is whether its convergence behavior is also strongly dependent on the physical outer BCs, and whether free space problems are also much easier to solve with multigrid than cavity problems. This is the motivation for our present study.

We use as our model problem the 1D Helmholtz equation

$$
\begin{aligned}
(\Delta + k^2)u &= f && \text{in } \Omega = (0,1),\\
\partial_x u - pu &= 0 && \text{at } x = 0,\\
\partial_x u + pu &= 0 && \text{at } x = 1,
\end{aligned}
\tag{1}
$$

where $k > 0$ is the wave number, and $f \in L^2(\Omega)$ is the source term. When the parameter $p = ik$, $i := \sqrt{-1}$, we obtain impedance BCs and the problem corresponds to a free space problem, while $p \to \infty$ leads to Dirichlet BCs and the problem is a cavity problem. We will compare the convergence behavior of domain decomposition and multigrid for these two situations.

Note that the simple 1D setting here allows us to explicitly derive Schwarz convergence factors and the basic two-grid operator for multigrid methods, and to optimize

Martin J. Gander
University of Geneva, Department of Mathematics, Switzerland, e-mail: martin.gander@unige.ch

Yafei Sun
Jilin University, School of Mathematics, China, e-mail: yafeisun@jlu.edu.cn

parameters and systematically perform numerical convergence analyses. Our results show that, unlike Schwarz methods, multigrid methods perform equally poorly for both 1D free space and cavity problems. Although for domain decomposition the 1D setting is a bit oversimplified, as the transparent boundary conditions become local, simple impedance conditions, and we thus use perturbations, the obtained results remain relevant for Schwarz methods in higher dimensions, as observed via semi-analytical Fourier analysis in [11]. We therefore expect that similar convergence differences also persist for multigrid methods applied to higher-dimensional Helmholtz problems. Moreover, while we only consider Dirichlet and Robin BCs here, the effects of mixed BCs could also be investigated analogously, where the interplay between absorbing and reflecting boundaries may further influence convergence properties. A rigorous analysis of such cases is left for future work.

2 Schwarz Domain Decomposition Methods for Helmholtz

We now introduce Schwarz domain decomposition methods for solving model (1). We only consider the case of two-subdomains, the case of multiple subdomains could be done following the techniques in [4]. We divide the computational domain $\Omega = (0,1)$ into two overlapping subdomains $\Omega_1 := (0,\beta)$ and $\Omega_2 := (\alpha,1)$ with overlap $L := \beta - \alpha > 0$. Then the optimized parallel Schwarz method starts from an initial guess $\{u_1^0, u_2^0\}$ and computes for $\ell \geq 1$ until convergence

$$\begin{array}{llll} (\Delta+k^2)u_1^\ell=f & \text{in } \Omega_1, & (\Delta+k^2)u_2^\ell=f & \text{in } \Omega_2, \\ \partial_x u_1^\ell - p u_1^\ell=0 & \text{at } x=0, & \partial_x u_2^\ell + p u_2^\ell=0 & \text{at } x=1, \\ \partial_x u_1^\ell + p_1 u_1^\ell=\partial_x u_2^{\ell-1}+p_1 u_2^{\ell-1} & \text{at } x=\beta, & \partial_x u_2^\ell - p_2 u_2^\ell=\partial_x u_1^{\ell-1}-p_2 u_1^{\ell-1} & \text{at } x=\alpha, \end{array} \tag{2}$$

where Robin transmission conditions $\partial_x + p_1$ and $\partial_x - p_2$ are imposed at the interfaces $x = \beta$ and $x = \alpha$. Here $p_1, p_2 \in \mathbb{C}$ are transmission parameters. The selection of them is typically guided by an analysis of the associated iteration operator, such as its spectral properties or convergence factors, to achieve rapid convergence. As discussed below, best performing parameter values can be identified directly from the explicit convergence factors in simplified settings like in 1D here, or via optimization techniques in more general situations; see e.g. [9, 10, 4, 11]. In the limit $p_1, p_2 \to \infty$, we obtain the classical parallel Schwarz method.

To analyze the convergence behavior of the parallel Schwarz method (2), we introduce the error $\hat{e}_j^\ell := u - u_j^\ell$, $j = 1,2$, which by linearity satisfies the same algorithm (2), but with zero data. Solving the ODEs in the corresponding error iteration, we obtain using the outer Robin BCs for each wave number k the solutions

$$\hat{e}_1^\ell(x) = A_1^\ell(k)\left(e^{ikx} + \tfrac{ik-p}{ik+p}e^{-ikx}\right),\ \hat{e}_2^\ell(x) = B_2^\ell(k)\left(e^{-ikx} + \tfrac{ik-p}{ik+p}e^{-ik(2-x)}\right).$$

To determine the two remaining constants $A_1^\ell(k)$ and $B_2^\ell(k)$ we insert the solutions into the Robin transmission conditions in (2), which leads to

$$
\begin{aligned}
A_1^\ell &= \frac{(p_1-ik)e^{-ik\beta}+(p_1+ik)\frac{ik-p}{ik+p}e^{-ik(2-\beta)}}{(p_1+ik)e^{ik\beta}+(p_1-ik)\frac{ik-p}{ik+p}e^{-ik\beta}} B_2^{\ell-1} =: \rho_1(k,p,p_1)B_2^{\ell-1},\\
B_2^\ell &= \frac{(p_2-ik)e^{ik\alpha}+(p_2+ik)\frac{ik-p}{ik+p}e^{-ik\alpha}}{(p_2+ik)e^{-ik\alpha}+(p_2-ik)\frac{ik-p}{ik+p}e^{-ik(2-\alpha)}} A_1^{\ell-1} =: \rho_2(k,p,p_2)A_1^{\ell-1}.
\end{aligned}
\tag{3}
$$

Let $\alpha^\pm := [\beta \pm (2-\beta)]/2$, $\beta^\pm := [\alpha \pm (2-\alpha)]/2$. From (3) we then get the convergence factor $\rho := \rho_1\rho_2$ of the parallel Schwarz method (2) to be

$$
\rho = \frac{(-pp_1-k^2)\sin(k\alpha^-)+(p_1k-pk)\cos(k\alpha^-)}{(pp_1-k^2)\sin(k\beta)+(p_1k+pk)\cos(k\beta)} \frac{(pp_2+k^2)\sin(k\alpha)+(p_2k-pk)\cos(k\alpha)}{(-pp_2+k^2)\sin(k\beta^-)+(p_2k+pk)\cos(k\beta^-)}. \tag{4}
$$

Adjusting the values of the parameters (p, p_1, p_2), we can obtain the convergence factors we are interested in (with overlap $L := \beta - \alpha$ in what follows):

$$
\rho_{\text{Cla}}^{\text{Cavity}} = \frac{\sin(k(\beta-1))\sin(k\alpha)}{\sin(k\beta)\sin(k(\alpha-1))}, \qquad (p = p_1 = p_2 \to \infty) \tag{5}
$$

$$
\rho_{\text{Opt}}^{\text{Cavity}} = \frac{(p_1\sin k(\beta-1)+k\cos k(\beta-1))(p_2\sin k\alpha - k\cos k\alpha)}{(p_1\sin k\beta + k\cos k\beta)(p_2\sin k(\alpha-1)-k\cos k(\alpha-1))}, \qquad (p\to\infty) \tag{6}
$$

$$
\rho_{\text{Cla}}^{\text{Free}} = e^{-ik2L}, \qquad (p = ik,\ p_1 = p_2 \to \infty) \tag{7}
$$

$$
\rho_{\text{Opt}}^{\text{Free}} = \frac{p_1-ik}{p_1+ik}\cdot\frac{p_2-ik}{p_2+ik}\cdot e^{-ik2L}. \qquad (p = ik) \tag{8}
$$

We see already that the classical Schwarz method for the free space problem does not converge, since the convergence factor $|\rho_{\text{Cla}}^{\text{Free}}| = 1$ in (7). A numerical investigation of the convergence behavior, together with that of multigrid, will be presented later.

3 Multigrid Methods for Helmholtz

Now for the multigrid method, we focus only on the two-grid case, as it serves as a fundamental component of the multigrid hierarchy. By discretizing problem (1) using a standard centered finite-difference scheme on a uniform mesh $\Omega^h := \{x_j = jh : j = 0, 1, \dots, N+1\}$, $h = \frac{1}{N+1}$, we obtain a linear system of the form $A\mathbf{u} = \mathbf{f}$ for approximating the solution $u_j \approx u(x_j)$. For the Dirichlet BC ($p \to \infty$), we have $\mathbf{u} = [u_1, u_2, \dots, u_N]$, $A = \frac{1}{h^2}\text{tridiag}\left(-1, 2-k^2h^2, -1\right)$ and $\mathbf{f} = \left(f(x_j)\right)_{j=1}^N$. For the Robin BC ($p = ik$), we need to include the boundary unknowns, $\mathbf{u} = [u_0, u_1, \dots, u_{N+1}]$, $\mathbf{f} = \left(f(x_j)\right)_{j=0}^{N+1}$, and by approximating the Robin BCs using a second-order centered finite difference with a ghost point, $\frac{u_{-1}-u_1}{2h} - iku_0 = 0$, $\frac{u_{N+2}-u_N}{2h} - iku_{N+1} = 0$, we get the corresponding discrete Helmholtz operator

$$
A = \frac{1}{h^2}\begin{bmatrix}
2-k^2h^2-i2kh & -2 & & & \\
-1 & 2-k^2h^2 & -1 & & \\
& \ddots & \ddots & \ddots & \\
& & -1 & 2-k^2h^2 & -1\\
& & & -2 & 2-k^2h^2-i2kh
\end{bmatrix}. \tag{9}
$$

We introduce the coarse grid $\Omega^H := \{x_j = jH : j = 0, 1, \ldots, n+1\}$ with $n = \frac{N-1}{2}$, $H = 2h$, and let A_H be the discrete Helmholtz operator on Ω^H like for A. Then, the two-grid method [1, 3, 7] for the linear system $A\mathbf{u} = \mathbf{f}$ is given by performing for $m = 0, 1, \ldots$

$$\begin{cases} \tilde{\mathbf{u}}^m := S^{\nu_1}(\mathbf{u}^m, \mathbf{f}); & \text{\% pre-smoothing} \\ \mathbf{r} := R(\mathbf{f} - A\tilde{\mathbf{u}}^m); & \text{\% restrict residual} \\ \mathbf{e} = A_H^{-1}\mathbf{r}; & \text{\% coarse-grid correction} \\ \tilde{\mathbf{u}}^{m+1} = \tilde{\mathbf{u}}^m + P\mathbf{e}; & \text{\% add coarse correction} \\ \mathbf{u}^{m+1} = S^{\nu_2}(\tilde{\mathbf{u}}^{m+1}, \mathbf{f}); & \text{\% post-smoothing} \end{cases} \tag{10}$$

where $\mathbf{u}^0$ is an initial guess, S^ν denotes ν iterations of a smoother S, P is a prolongation operator, and R is a restriction operator, which will be defined more precisely below. The two-grid algorithm (10) is a stationary iterative method, and its iteration matrix (also called the *two-grid operator*) is given by [1]

$$T = S^{\nu_2} C S^{\nu_1} = S^{\nu_2}\left(I - PA_H^{-1}RA\right)S^{\nu_1}. \tag{11}$$

To achieve a fast-converging two-grid algorithm (10), an efficient smoother and coarse grid correction are required. Inspired by the techniques proposed in [7], we consider using a multi-step damped Jacobi smoother consisting of multiple consecutive smoothing steps, each with its own damping parameter $\omega_i, i = 1, \ldots, s$,

$$\begin{cases} \bar{\bar{\mathbf{u}}}^1 = \mathbf{u}^m + \omega_s D^{-1}(\mathbf{f} - A\mathbf{u}^m) = (I - \omega_s D^{-1}A)\mathbf{u}^m + \omega_s D^{-1}\mathbf{f}, \\ \bar{\bar{\mathbf{u}}}^2 = \bar{\bar{\mathbf{u}}}^1 + \omega_{s-1} D^{-1}(\mathbf{f} - A\bar{\bar{\mathbf{u}}}^1) = (I - \omega_{s-1} D^{-1}A)\bar{\bar{\mathbf{u}}}^1 + \omega_{s-1} D^{-1}\mathbf{f}, \\ \vdots \\ \mathbf{u}^{m+1} = \bar{\bar{\mathbf{u}}}^{s-1} + \omega_1 D^{-1}(\mathbf{f} - A\bar{\bar{\mathbf{u}}}^{s-1}) = (I - \omega_1 D^{-1}A)\bar{\bar{\mathbf{u}}}^{s-1} + \omega_1 D^{-1}\mathbf{f}, \end{cases} \tag{12}$$

where $D := \mathrm{diag}(A)$ and $\mathbf{u}^m$ is the calculated approximate solution at iteration m. The corresponding iteration matrix is $S_{\omega_1,\ldots,\omega_s} := (I - \omega_1 D^{-1}A)(I - \omega_2 D^{-1}A)\cdots(I - \omega_s D^{-1}A)$. Note that when $s = 1$, we obtain the classical damped Jacobi iteration, and $s = 2$ leads to the two-step damped Jacobi iteration studied in [7].

For the coarse-grid correction $C = I - PA_H^{-1}RA$, we use the standard linear interpolation for P and the full weighting restriction for R. Their matrix representations are provided in [7, Eq. (3.1), Eq. (3.4)]. Such a standard coarse-grid correction is however insufficient to produce an efficient two-grid algorithm for the Helmholtz equation: as shown in [7, Section 3.2] for the case of Dirichlet BCs, the eigenvalues of this coarse-grid correction operator C have a pole near a certain frequency index $\bar{j}$ whenever the product of the wave number k and the mesh size h satisfies $kh \leq 1$, thereby amplifying the associated error component. To alleviate this issue, a shifted wave number $\tilde{k}$, derived from dispersion correction, was introduced on the coarse grid in [7, 3] to reduce the phase error and stabilize the coarse-grid correction, and was shown to be essential for constructing efficient multigrid solvers. Here, we adopt a similar strategy; however, instead of using the tailored $\tilde{k}$ from [7, 3], we treat the modified wave number $\tilde{k}$, along with the damping parameters ω_i, as free parameters, and our goal is to determine the best values of $\tilde{k}$ and ω_i to yield the most efficient two-grid algorithm. We do this by numerically solving the min–max problem

$$\min_{\omega_i \in \mathbb{C}, \tilde{k} \in \mathbb{R}} \max_j \left|\lambda_j\left(T\right)\right|, \quad T = S^{\nu_2}_{\omega_1,\ldots,\omega_s}\left(I - P\left(A_H(\tilde{k})\right)^{-1} RA(k)\right) S^{\nu_1}_{\omega_1,\ldots,\omega_s}, \quad (13)$$

where $A_H(\tilde{k})$ indicates that the dispersion correction has been incorporated by introducing the undetermined shifted wave number $\tilde{k}$ on the coarse grid. In higher dimensions, solving the associated min-max problem (13) is still possible, but deriving the two-grid operator is technically more involved, and dispersion correction typically requires more sophisticated discretizations or specialized stencils; see, e.g., [2]. Extending the present study to these cases is left for future work.

For both cavity and free space problems, we now have the Schwarz convergence factors $\rho(k, p, p_1, p_2)$ (see Eqs. (5)-(8)) and the two-grid operator T (see Eq. (11)). We show in the next section a comprehensive numerical comparison of the convergence behaviors of these two iterative methods for cavity and free space problems.

4 Numerical Comparison of Schwarz and Multigrid

To evaluate and compare the performance of the Schwarz domain decomposition and multigrid methods, we examine the convergence behavior of both algorithms with respect to the original wave number k. For the two-grid method, two-step and four-step damped Jacobi smoothers with different numbers of smoothing steps ($\nu = \nu_1 + \nu_2$) are used. Here we use the same number of pre- and post-smoothing steps, $\nu_1 = \nu_2$, and $N = 31$, $h = \frac{1}{N+1} = \frac{1}{32}$, $n = \frac{N-1}{2} = 15, H = \frac{1}{n+1} = 2h = \frac{1}{16}$. Additionally, since our goal is to ensure convergence over a wide range of wave numbers–particularly those that may occur within a full multigrid cycle–we select a specific sequence of wave numbers by placing k^2 exactly between two Dirichlet eigenvalues[1], namely, for the given N and h, $k := \{k_1, \ldots, k_N, k_N + k_1, \ldots, 2k_N\}$ with $k_l = \sqrt{\frac{2}{h^2}\left(\sin^2\frac{(l-1)\pi h}{2} + \sin^2\frac{l\pi h}{2}\right)}, l = 1, \ldots, N$. For the Schwarz methods we consider a symmetric two-subdomain decomposition of $\Omega := (0, 1)$ with $\Omega_1 = (0, \beta) := (0, \frac{1}{2} + \frac{L}{2})$, $\Omega_2 = (\alpha, 1) := (\frac{1}{2} - \frac{L}{2}, 1)$, where the overlap is $L = \beta - \alpha = 0.002$, and convergence is examined on a finer grid of wave numbers $k \in (0, 100]$.

Note that for the OSM, we can determine the best transmission parameters by enforcing the numerators of $\rho^{\text{Cavity}}_{\text{Opt}}$ and $\rho^{\text{Free}}_{\text{Opt}}$ (see Eq. (6) and Eq. (8)) to vanish. This yields $p^{\text{Cavity}}_{1,*} = -\frac{k}{\tan k(\beta-1)}$, $p^{\text{Cavity}}_{2,*} = \frac{k}{\tan k\alpha}$, $p^{\text{Free}}_{1,*} = p^{\text{Free}}_{2,*} = ik$, and by using these best parameters, the OSM converges in two iterations, effectively acting as a direct solver on the whole domain. However, these best choices are practical only in 1D, where $p_{1,*}$ and $p_{2,*}$ are scalar values for a given wavenumber k. In contrast, in higher dimensions, directly forcing the convergence factor to vanish results in

[1] This prevents the potential singularity induced by the Dirichlet boundary condition.

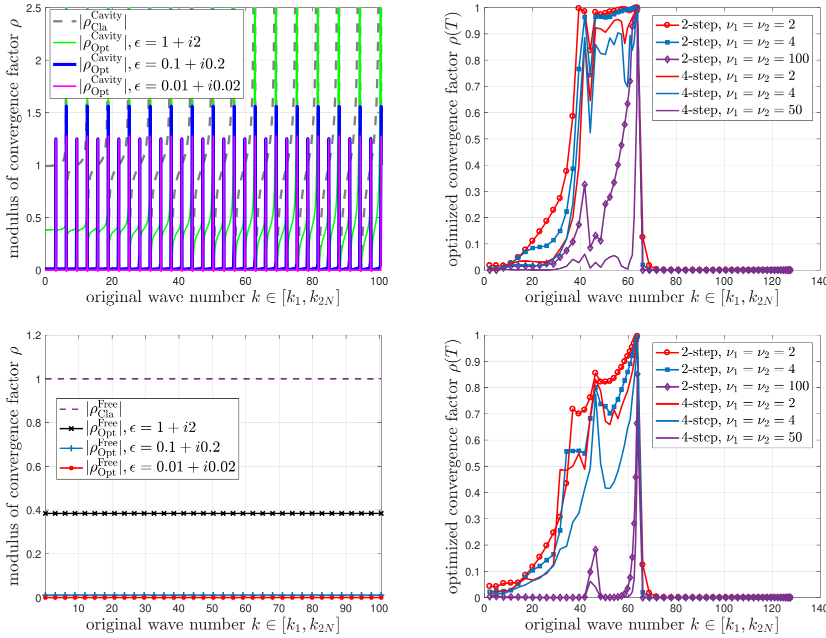

Fig. 1 Convergence factors as functions of the wave number k. Top left: Schwarz methods with approximated best parameters (see Eq. (14)) for the cavity. Top right: Two-grid methods for the cavity. Bottom left: Schwarz methods with approximated best parameters (see Eq. (14)) for the free space problem. Bottom right: Two-grid methods for the free space problem.

optimal transmission parameters that correspond to nonlocal operators, making them impractical to implement. The best one can do in higher dimensions is to get an approximation of these optimal parameters [9, 11]. In order to faithfully reproduce the scenario in which approximate techniques are used in higher dimensions to approximate the optimal operators for computational feasibility, we do not use the optimal parameters directly here; instead, we use a slight perturbation of them to represent their approximations, namely (note that for the symmetric decomposition in this example, the optimal $p_{1,*}^{\text{Cavity}}, p_{2,*}^{\text{Cavity}}$ have the same values $\frac{k}{\tan k\alpha}$)

$$p_{1,\text{app}}^{\text{Cavity}} = p_{2,\text{app}}^{\text{Cavity}} = \frac{k}{\tan k\alpha}(1+\epsilon), \quad p_{1,\text{app}}^{\text{Free}} = p_{2,\text{app}}^{\text{Free}} = ik(1+\epsilon), \quad \epsilon \in \mathbb{C}. \tag{14}$$

To study how the Schwarz and two-grid methods contract for the cavity problem, the first row of Fig. 1 shows the convergence factors as functions of wave number k. From the results on the top left, we see that for the cavity problem, the classical Schwarz method exhibits rapid divergence for many wave numbers k. The OSM with perturbed parameters (14) also shows convergence difficulties: even a very small perturbation ($\epsilon = 0.01 + i0.02$) can cause convergence problems for certain k, which worsen rapidly as the perturbation increases. This indicates that in the cavity case, the optimal transmission condition is highly sensitive to perturbations, and even a relatively accurate approximation may lead to severe convergence degradation. The reason for the pronounced oscillations is that the fully reflecting outer boundary traps wave energy, leading to repeated reflections and cavity resonances. When these resonant modes interact with the Schwarz transmission conditions, errors are amplified rather than transported out of the domain, leading to rapid divergence. In terms of the convergence factor (6), this corresponds to near-singularities from zeros of its denominator. Although exact cavity resonance frequencies, i.e., those zeros, are $k_n = n\pi$, for which the convergence factor is shown to be identically equal to 1, the interaction between transmission conditions and the fully reflecting boundary shifts them to nearby values $\tilde{k}_n = n\pi + \delta_n$, causing the observed oscillations. These accurate $\tilde{k}_n$ are determined by a transcendental equation, and are not pursued here.

The two-grid method shows similar convergence difficulties for the cavity problem, as seen in Fig. 1 on the top right, where the convergence factor remains close to 1 for wave numbers k between approximately $\hat{k} = \sqrt{2}/h$ and k_N. While additional smoothing steps sightly reduce the convergence factor, the improvement near k_N remains very limited. Preliminary numerical experiments indicate that some eigenvalues of the Jacobi smoother, associated with high-frequency error components, are close to one and approach unity as the wavenumber nears k_N. This suggests that the observed deterioration is closely related to the reduced smoothing effectiveness of the Jacobi relaxation. A rigorous analysis of this behavior is left for future work.

In the second row of Fig. 1 we present the corresponding results for the free space problem, i.e., those with impedance outer BCs. We see on the bottom left that, while the classical Schwarz method still fails to converge, the OSM with approximated best parameters (14) converges rapidly and robustly for all wave numbers. This indicates that for the free space problem, the transparent transmission condition is robust to perturbations, and that the OSM can achieve fast convergence even with a relatively rough approximation of the optimal parameters. In sharp contrast to the OSM, the two-grid method shows no substantial improvement in convergence compared to the cavity case, as illustrated in Fig. 1 on the bottom right. There still remain certain wave numbers k (particularly those around k_N) for which the two-grid method struggles to converge.

We focused our presentation here on the Jacobi smoother, but we have also tested several other standard smoothers (e.g., Kaczmarz and even GMRES) and observed similar results. Furthermore, in addition to the theoretically optimized convergence factors shown in Fig. 1, we also measured the actual numerical convergence factors. Some representative results are shown in Table 1, from which we also observe a clear difference in how outer boundary conditions affect the convergence of Schwarz and two-grid methods. For Schwarz methods, convergence is much better for the free space problem than for the cavity problem, whereas for the two-grid method both cavity and free space problems remain equally hard to be solved. While it was shown in [11] for higher dimensional Helmholtz problems why optimized Schwarz methods work much better for free space problems than for cavity (and wave guide) problems, it is currently not understood which free space problems are equally hard

Table 1 Numerical convergence factors for Schwarz and multigrid methods

Alg. / k	OSM (cavity) $\epsilon = 1 + i2$	OSM (free space) $\epsilon = 1 + i2$	Two-grid (cavity) 2-step, $\nu_1 = \nu_2 = 4$	Two-grid (free space) 2-step, $\nu_1 = \nu_2 = 4$
2.3	0.6201	0.6194	0.0078	0.0277
18.72	0.9401	0.6198	0.0844	0.0938
18.76	1.1201 (div.)	0.6157	0.0843	0.0903
60	0.4715	0.6200	0.9944 (slow)	0.8676 (slow)
62.4	0.9255	0.6193	0.9922 (slow)	0.9423 (slow)
62.6	1.3099 (div.)	0.6179	0.9914 (slow)	0.9492 (slow)
72.2	0.9092	0.6187	1.1405e-05	1.1323e-05
72.3	1.1600 (div.)	0.6193	1.0365e-05	1.0283e-05

for multigrid methods like cavity problems. Explaining this and finding a remedy is our current focus of research.

References

1. Cocquet, P.H., Gander, M.J.: How large a shift is needed in the shifted Helmholtz preconditioner for its effective inversion by multigrid? SIAM J. Sci. Comput. **39**(2), A438–A478 (2017)
2. Cocquet, P.H., Gander, M.J., Xiang, X.: A finite difference method with optimized dispersion correction for the Helmholtz equation. In: International Conference on Domain Decomposition Methods, pp. 205–213. Springer (2017)
3. Cocquet, P.H., Gander, M.J., Xiang, X.: Dispersion correction for Helmholtz in 1D with piecewise constant wavenumber. In: International Conference on Domain Decomposition Methods, pp. 359–366. Springer (2018)
4. Dolean, V., Gander, M.J., Kyriakis, A.: Closed form optimized transmission conditions for complex diffusion with many subdomains. SIAM J. Sci. Comput. **45**(2), A829–A848 (2023)
5. Engquist, B., Ying, L.: Sweeping preconditioner for the Helmholtz equation: Moving perfectly matched layers. Multiscale Model. Sim. **9**(2), 686–710 (2011)
6. Erlangga, Y.A., Oosterlee, C.W., Vuik, C.: A novel multigrid based preconditioner for heterogeneous Helmholtz problems. SIAM J. Sci. Comput. **27**(4), 1471–1492 (2006)
7. Ernst, O.G., Gander, M.J.: Multigrid methods for Helmholtz problems: A convergent scheme in 1D using standard components. In: I.G. Graham, U. Langer, J.M. Melenk, M. Sini (eds.) Direct and Inverse Problems in Wave Propagation and Applications, pp. 135–186. De Gruyter (2013)
8. Gander, M.J., Graham, I.G., Spence, E.A.: Applying GMRES to the Helmholtz equation with shifted Laplacian preconditioning: what is the largest shift for which wavenumber-independent convergence is guaranteed? Numer. Math. **131**(3), 567–614 (2015)
9. Gander, M.J., Magoules, F., Nataf, F.: Optimized Schwarz methods without overlap for the Helmholtz equation. SIAM J. Sci. Comput. **24**(1), 38–60 (2002)
10. Gander, M.J., Zhang, H.: A class of iterative solvers for the Helmholtz equation: Factorizations, sweeping preconditioners, source transfer, single layer potentials, polarized traces, and optimized Schwarz methods. SIAM Rev. **61**(1), 3–76 (2019)
11. Gander, M.J., Zhang, H.: Schwarz methods by domain truncation. Acta Numer. **31**, 1–134 (2022)
12. Stolk, C.C.: A rapidly converging domain decomposition method for the Helmholtz equation. J. Comput. Phys. **241**, 240–252 (2013)
13. Stolk, C.C., Ahmed, M., Bhowmik, S.K.: A multigrid method for the Helmholtz equation with optimized coarse grid corrections. SIAM J. Sci. Comput. **36**(6), A2819–A2841 (2014)